Laser-Light-Scattering Study of Internal Motions of Polymer Chains Grafted on Spherical Latex Particles

Cheng Yang,[†] Jayachandran N. Kizhakkedathu,[‡] Donald E. Brooks,[‡] Fan Jin,[§] and Chi Wu*[,§,#]

Department of Chemical and Material Engineering, Southern Yangtze University, Wuxi, Jiangsu, People's Republic of China, Department of Pathology and Chemistry, The University of British Columbia, Vancouver, British Columbia, Canada, Department of Chemistry, The Chinese University of Hong Kong, Shatin N.T., Hong Kong, and The Open Laboratory of Bond Selective Chemistry, Department of Chemical Physics, University of Science and Technology of China, Hefei, Anhui, People's Republic of China

Received: June 16, 2004; In Final Form: August 19, 2004

Using atom-transfer radical polymerization, we have prepared core−shell particles by grafting thermally sensitive poly(*N*-isopropylacrylamide) (PNIPAM) chains on a spherical polystyrene latex core (with a radius of ∼287 nm) via the "grafting-from" approach. As the temperature increases from 25 °C to 35 °C, the PNIPAM shell shrinks from a thickness of 625 nm to 110 nm and the chain density near the core increases from 7.3 × 10^{-3} g/cm^3 to 7.2 × 10^{-2} g/cm^3. Using such core−shell particles, we have, for the first time, been able to study dynamics of long chains anchored on a particle in dilute dispersion by laser-light scattering. Our results showed that, besides the translational diffusion of the particle as a whole, there also exists an additional slow relaxation mode that is only observable at larger scattering vectors (q),which are presumably related to internal motions of the shell. In the fully swollen state, the relaxation rate of the slow motion ($\langle\Gamma\rangle_{slow}$) is insensitive to the observation length ($1/q$); however, its contribution to the scattering intensity (A_{slow}) increases as q increases. In the shrunken state, $\langle\Gamma\rangle_{slow}$ slightly decreases as q increases. $\langle\Gamma\rangle_{slow}$ can be scaled to the shell thickness ($\langle L\rangle_{brush}$) as $\langle\Gamma\rangle_{slow} \propto \langle L\rangle_{brush}^{\alpha}$, with $\alpha = -2.5 \pm 0.2$, which is smaller than the predicated value of 3.

Introduction

Grafting long polymer chains on a surface can result in a polymer brush if the grafting density is sufficiently high. Polymer brushes have attracted much attention, because of their many useful implications, such as applications in wetting, adhesion, colloid stability, and biocompatibility. Fundamentally, grafted chains represent a constrained structure, wherein osmotic repulsion and elastic energy are in balance. Alexander[1] and de Gennes[2] studied the conformation of chains grafted on an impermeable planar surface in good solvent, using the scaling approach. Later, Milner and Witten[3] and Birshtein et al.[4] used the self-consistent field method to describe the conformation of grafted chains. It is helpful to note that, in this aspect, the theory[1−10] is much more advanced than experimental studies,[11−19] because it is rather difficult, if not impossible, to prepare densely grafted chains with a uniform length.

Many theoretical studies of dynamics of polymer brushes have been reported;[20−23] however, so far, direct experimental investigations have been limited,[24−29] partially because of difficulties in the preparation of polymer brushes and partially due to weak scattering of the grafted layer, in comparison with the substrate. Farago et al.[25] investigated the shell dynamics of a core−shell micelle by neutron spin−echo spectroscopy. They attributed the peculiar multi-relaxation modes to the breathing of the shell on the basis of the idea that the grafted chains in the shell are actually in the semidilute regime with a varying concentration profile. Fytas et al.[26] studied the dynamics of polystyrene (PS) chains anchored on a flat surface with evanescent wave dynamic light scattering and found that the chain dynamics was related to thermal fluctuation of the segment density profile of the brushlike layer. They showed that there was a preferred wavelength of order L_0 (layer thickness) of the fluctuation with a concurrent slowing of the thermal decay rate. Furthermore, they investigated the chain dynamics of polymer brushes in concentrated solution or dispersion by dynamic light scattering.[27−29] Three relaxation modes were determined for the multiarm star polymer, namely (i) the fast cooperative diffusion for the entangled arms, (ii) the diffusion of the star polymer as a whole, and (iii) the so-called structural mode, which corresponds to a rearrangements of the star chains orderly packed in the semidilute regime. However, no fast cooperative diffusion of the entangled chains in the shell was observed for giant core−shell micelles. Instead, some collective motions of the chains in the swollen shell were observed at higher scattering angles.

In the dilute regime, only diffusive relaxation was observed for both the star polymers and giant polymeric micelles, even at the highest scattering angle. This is because the chains are still relatively shorter than the observation length ($1/q$), where $q = (4\pi n/\lambda_0)\sin(\theta/2)$ is the scattering vector (where n is the refractive index of the solvent, λ_0 the laser wavelength in a vacuum, and θ the scattering angle). To our knowledge, internal motions of long polymer chains grafted on a particle surface in dilute dispersion have not been observed yet. In this paper, using the atom-transfer radical polymerization (ATRP) method and a "grafted-from" approach,[30−33] thermally sensitive, ultralong

* Author to whom correspondence should be addressed. Telephone: 852-2609-6106. Fax: 852-2603-5057. E-mail address: chiwu@cuhk.edu.hk.
[†] Southern Yangtze University.
[‡] The University of British Columbia.
[§] The Chinese University of Hong Kong.
[#] University of Science and Technology of China.

10.1021/jp047403w CCC: $27.50
Published on Web 11/09/2004

poly(*N*-isopropylacrylamide) (PNIPAM) chains were grafted on the surface of a PS latex core to form a core−shell structure. The hydrodynamic thickness of the PNIPAM shell (brush), swollen in pure water at low temperatures, reaches ∼700 nm. More importantly, the thickness of such a brush can continuously vary with the dispersion temperature in the range of 25−35 °C. This makes such a model system ideal for the investigation of chain dynamics of polymer brushes.

Experimental Section

Sample Preparation. The preparation of PNIPAM−PS core−shell particles was previously detailed.[32] All commercial reagents were purchased from Aldrich and used without further purification. Analytical thin-layer chromatography (TLC) was performed on commercial Whatman flexible plates coated with 250-μm-thick silica gel. Styrene (Aldrich, 99%) was first washed with a 1% NaOH solution and then distilled under reduced pressure. *N*-isopropylacrylamide (NIPAM) (Aldrich, 99%) was purified by recrystallization from *n*-hexane and stored under argon at −20 °C until use. 2-(2′-Chloropropionato)ethyl acrylate (HEA-Cl) was synthesized by the method described in our earlier report.[32] Narrowly dispersed PS latex seeds were prepared by surfactant-free emulsion polymerization and characterized by following the reported procedure.[32] The average hydrodynamic radius of these narrowly distributed seeds was ∼287 nm, as measured by a particle size analyzer.

To prepare a shell made of grafted PNIPAM chains, we first synthesized a layer of ATRP initiator. A suspension of PS latex seeds (3.33 wt %, 523 g) was heated to 70 °C. The suspension was stirred, degassed, and purged with argon. Styrene (5.2 g, 0.05 mol) and HEA-Cl (3.5 g, 0.017 mol) were added successively to the suspension in a 10-min interval. The initiator solution (0.2 g, 0.74 mmol of potassium persulfate (KPS) in 30 mL of water, degassed) was added after 5 min. The reaction was continued for 6 h, and the latex was cleaned by dialysis against water for 1 week and five cycles of centrifugation and redispersion. Functional latex particles were characterized by conductometric titration, ^{1}H NMR, and particle size analysis, as described earlier.[32,33] The average hydrodynamic radius of such obtained narrowly distributed latex particles is ∼287 nm.

The grafting of PNIPAM was then conducted in a glovebox that was filled with argon, because of the air sensitivity of the Cu(I) complex. A suspension of latex (22 g) carrying the ATRP initiator layer was degassed for 2.5 h by continuous vacuum and argon cycles and then transferred to the glovebox. Brij-35 (nonionic surfactant) (0.035 g, 0.16 wt %) was added to the suspension and stirred for 5 min. A mixture of NIPAM (0.285 g, 2.5 mmol), 1,1,4,7,10,10-hexamethyltriethylenetetramine (HMTETA) (37 μmol), CuCl (15 μmol), $CuCl_2$ (3.0 μmol), and copper powder (16 μmol) was stirred for 3 min to form a solution. A quantity (3.5 g) of Brij-35 stabilized PS latex seeds was added under stirring at 22 °C. The grafting reaction was continued for 24 h. The resultant core−shell particles were cleaned by repeated sequential centrifugation and redispersion in water, sodium persulfate ($NaHSO_3$) solution (50 mmol), and water, to remove adsorbed copper complexes for 8−10 cycles until there was no detectable amount of polymer/monomer/catalyst in the supernatant. To characterize the molar mass and grafting density of the grafted chains (GPC-MALLS), the grafted chains were cleaved from the latex surface by quantitative saponification.[32,33] The grafting density was $\sim 4.5 \times 10^{-8}$ mol/m^2 and the number-averaged molar mass (M_n) of the grafted PNIPAM chains was 8.37×10^5 g/mol, with a polydispersity index of $M_w/M_n \approx 1.28$ (where M_w is the weighted-averaged molecular mass).

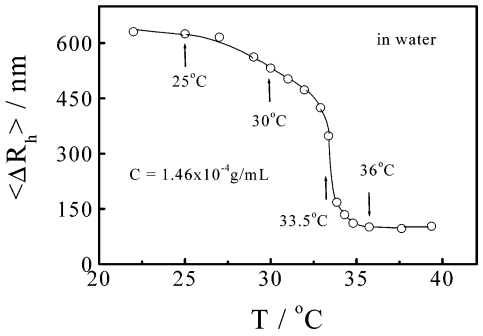

Figure 1. Temperature dependence of average hydrodynamic thickness ($\langle \Delta R_h \rangle$) of the poly(*N*-isopropylacrylamide) (PNIPAM) shell of a core−shell particle, where $\langle \Delta R_h \rangle = \langle R \rangle_h - \langle R \rangle_{n,c}$ with $\langle R \rangle_h$ and $\langle R \rangle_{n,c}$ being the average hydrodynamic radius of particle with and without the grafted chains, respectively.

Laser-Light Scattering. A modified commercial laser-light-scattering (LLS) spectrometer (model ALV/SP-125) was used, which was equipped with a Uniphase model ALV-5000 multi-τ digital time correlator and a He−Ne laser (output power of ∼22 mW at a wavelength of $\lambda = 632.8$ nm). In static LLS, angular dependence of the excess absolute time-average scattered intensity, which is known as the Rayleigh ratio $R_{vv}(q)$, was measured. In dynamic LLS, the intensity−intensity time correlation function $G^2(t,q)$ in the self-beating mode was measured, where t is the delay time. $G^{(2)}(t,q)$ can be related to the normalized first-order electric-field−electric-field time correlation function $|g^{(1)}(t,q)| = [\langle E(0,q)E^*(t,q)\rangle]$ as[34]

$$G^{(2)}(t,q) = \langle I(0,q)I(t,q)\rangle = A[1 + \beta|g^{(1)}(t,q)|^2] \qquad (1)$$

where A is the measured baseline ($A = \langle I(0)\rangle^2$) and β is the coherent factor, depending on the detection optics. For a broadly distributed system, $|g^{(1)}(t,q)|$ is related to a characteristic relaxation (decay) time distribution $G(t)$, as

$$|g^{(1)}(t,q)| = \int_0^\infty G(t) \exp\left(-\frac{t}{\tau}\right) d\tau \qquad (2)$$

$G(t)$ can be calculated from the Laplace inversion of each measured $G^{(2)}(t,q)$, on the basis of eqs 1 and 2. For a pure diffusive relaxation, $(\Gamma/q^2)_{q\to 0, C\to 0}$ leads to the translational diffusion coefficient D, which is further related to the hydrodynamic radius R_h by the Stokes−Einstein equation: $R_h = k_B T/(6\pi\eta D)$, where k_B is the Boltzmann constant, T the absolute temperature, and η the solvent viscosity. The dilute dispersion used was prepared by adding a 2.8% core−shell latex dispersion into a dust-free light-scattering cell with a desired amount of dust-free deionized water. The final concentration was 1.46×10^{-4} g/mL.

Results and Discussion

Figure 1 shows the decrease of the average hydrodynamic radius $\langle R_h \rangle$ of the PS−PNIPAM core−shell particles with increasing temperature, especially in the range of 33−34 °C. It is helpful to note that linear PNIPAM chains free in water have a low critical solution temperature (LCST) of ∼32 °C. The grafted chains clearly have a slightly higher LCST value, presumably because the close packing of the grafting chains on the surface hinders the chain shrinkage. Note that the PS core is temperature-insensitive in this range. Figure 1 clearly reveals that the chains grafted on the core are in the swollen

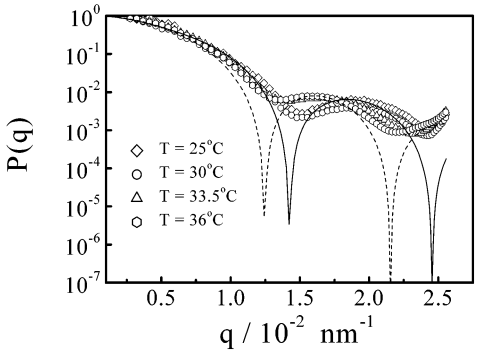

Figure 2. Static structural factor curve of the core−shell particles. The continuous line represents calculation with a core thickness of R_c = 287 nm and shell thickness of R = 912 nm, and the dashed line represents calculation a core thickness of R_c = 287 nm and a shell thickness of R = 397 nm.

state at 25 °C but fully collapse at ∼36 °C. In the range of 25−35 °C, the shell thickness decreases from 625 to 110 nm, corresponding to a change of ∼21 times that of the average chain density of the shell. Note that, for linear swollen PNIPAM chains with a similar molar mass free in water at 25 °C, the $\langle R_h \rangle$ value is only ∼35 nm. The shell thickness reveals that, even in the fully collapsed state, the chains grafted on the surface are still squeezed and elongated, because of the high grafting density. It is also helpful to note that the chain density is not uniform in the shell, especially in the swollen state.

Figure 2 shows the intensity profiles of the light scattered from the core−shell particles at different temperatures. The positions of the two minimums of $P(q)$ gradually shift to a lower q value with increasing temperature. The theory of spherical brushes was derived by Daoud and Cotton.[5,14] The density profile ($\rho(r)$) of a star with f arms can be described as follows:

$$\rho(r) \approx f^{(3\nu-1)/2\nu} r^{(1-3\nu)/\nu} \tag{3}$$

where we assume that each arm has a Flory exponent ν. For a uniform core, $\rho(r) \approx \rho_c$; a brush in the theta solvent is represented as $\rho(r) \approx r^{-1}$, and a swollen brush in a good solvent is represented as $\rho(r) \approx r^{-4/3}$. In the present case, especially near the theta temperature (∼30.6 °C), we approximated $\rho(r)$ by the following density profile: $\rho(r) = \rho_c$ when $r \le R_c$ and $\rho(r) \approx \rho_0 r^{-1}$ when $R_c \le r \le R$, where ρ_0 is the surface chain density at the surface of the core, and R_c and R are the radii of the core and the particle, respectively. The form factor of the core−shell particle can be derived as follows:

$$\begin{aligned} P_{\text{core-shell}}(q) &= \left[\frac{\int_0^R b(r)\rho(r)\frac{\sin(qr)}{qr} r^2\,\mathrm{d}r}{\int_0^R b(r)\rho(r) r^2\,\mathrm{d}r}\right]^2 \\ &= \left[\frac{\int_0^{R_c} b_c\rho_c\frac{\sin(qr)}{qr} r^2\,\mathrm{d}r + \int_{R_c}^R b_s\rho_0 r^{-1}\frac{\sin(qr)}{qr} r^2\,\mathrm{d}r}{\int_0^{R_c} b_c\rho_c r^2\,\mathrm{d}r + \int_{R_c}^R b_s\rho_0 r^{-1} r^2\,\mathrm{d}r}\right]^2 \\ &= \left[\frac{2b_c\rho_c R_c^3[P_{\text{core}}(q)]^{1/2} + 3b_s\rho_0(R^2 - R_c^2)[P_{\text{shell}}(q)]^{1/2}}{2b_c\rho_c R_c^3 + 3b_s\rho_0(R^2 - R_c^2)}\right]^2 \end{aligned} \tag{4}$$

where

$$[P_{\text{core}}(q)]^{1/2} = \frac{3[\sin(qR_c) - (qR_c)\cos(qR_c)]}{(qR_c)^3}$$

$$[P_{\text{shell}}(q)]^{1/2} = \frac{2[\cos(qR_c) - \cos(qR)]}{q^2(R^2 - R_c^2)}$$

and $b(r)$ is a constant for a given polymer and solvent, because it is related to differential refractive index increments. Considering that the core and the shell are composed of two different polymers, we set the following: for $r \le R_c$, $b(r) = b_c$; and for $R_c \le r \le R$, $b(r) = b_s$. Note that ρ_c and ρ_0 are related to the masses of the core and shell (M_c and M_s, respectively), by

$$M_c = 4\pi\int_0^{R_c}\rho_c r^2\,\mathrm{d}r = \frac{4}{3}\pi R_c^3\rho_c \qquad \left(\text{or } \rho_c = \frac{3M_c}{4\pi R_c^3}\right) \tag{5a}$$

and

$$\begin{aligned} M_s &= 4\pi\int_{R_c}^R \rho(r) r^2\,\mathrm{d}r \\ &= 2\pi\rho_0(R^2 - R_c^2) \qquad \left(\text{or } \rho_0 = \frac{M_s}{2\pi(R^2 - R_c^2)}\right) \end{aligned} \tag{5b}$$

The estimate of $\rho(R_c)$ changes from 7.3×10^{-3} g/cm^3 to 7.2×10^{-2} g/cm^3 when the temperature increases from 25 °C to 36 °C. Using eq 5, we can rewrite eq 4 as

$$\begin{aligned} P_{\text{core-shell}}(q) &= \left[\frac{b_c M_c[P_{\text{core}}(q)]^{1/2} + b_s M_s[P_{\text{shell}}(q)]^{1/2}}{b_c M_c + b_s M_s}\right]^2 \\ &= [B_{\text{core}}[P_{\text{core}}(q)]^{1/2} + B_{\text{shell}}[P_{\text{shell}}(q)]^{1/2}]^2 \end{aligned} \tag{6}$$

where $B_{\text{core}} = b_c M_c/(b_c M_c + b_s M_s)$, $B_{\text{shell}} = b_s M_s/(b_c M_c + b_s M_s)$, and $B_{\text{core}} + B_{\text{shell}} = 1$. In the calculation, we try to choose a proper value of B_{shell} to fit all the scattering profiles measured at different temperatures. Note that the fitting is not perfect, because we only estimate the chain density profile in the calculation. However, this will not affect what we try to discuss in this paper.

Figure 3 shows the scattering vector (q) and temperature (T) dependence of the measured intensity−intensity time correlation functions of the core−shell particles in a dilute dispersion, where the delay time (t) has been scaled by q^2. The four temperatures used here are marked in Figure 1 by arrows. If the relaxation is purely diffusive, the measured time correlation functions should be superimposed on each other. As shown in Figure 3, those measured at lower scattering angles have only one relaxation mode and are indeed overlapping with each other. With increasing scattering angle θ, another slow relaxation mode appears at longer delay times. Note that $1/q$ in LLS represents an observation length. The change of θ from 15° to 154° corresponds to a change of $1/q$ from 290 nm to 39 nm. With increasing q, the light gradually probes the local dynamics of long chains. The appearance of the slow relaxation at higher scattering angles indicates some slow local motions of the grafted chains, because the spherical hard PS core has no internal motion.

However, there is another possibility for such a slow mode, namely, the refraction from the existing window or cuvette wall. Bantle et al.[35] showed that the reflected beam could lead to a slow mode, and the correlation function of monodis-

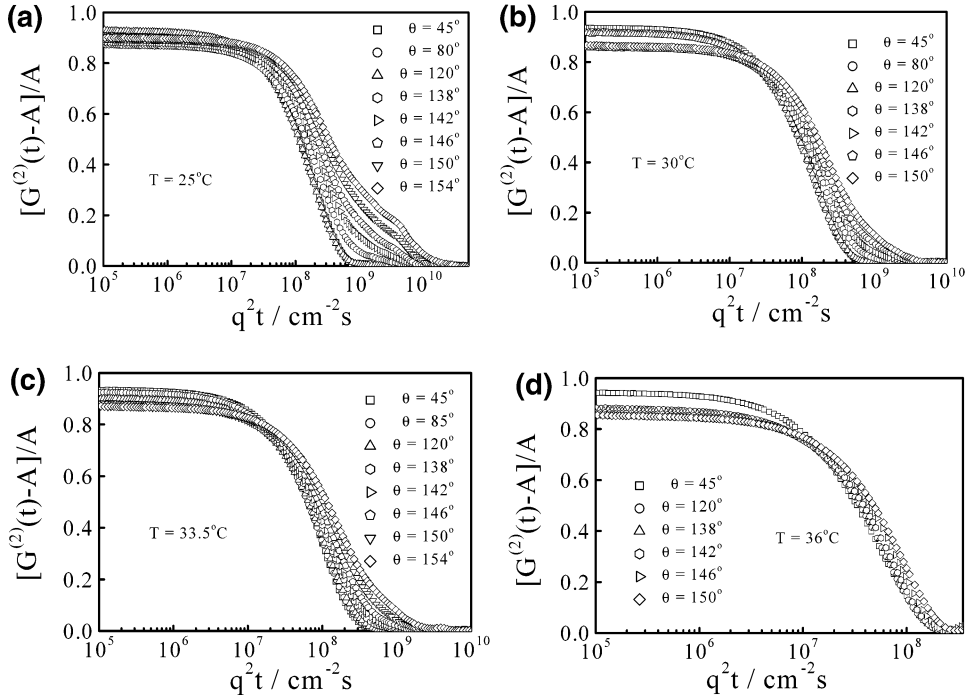

Figure 3. Intensity−intensity time correlation functions of a core−shell particle in water at different temperatures: (a) 25, (b) 30, (c) 33.5, and (d) 36 °C.

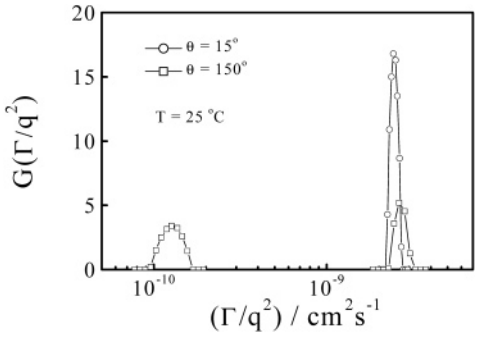

Figure 4. Scattering-vector-corrected characteristic linewidth distributions ($G(\Gamma/q^2)$) of core−shell particles in water at 25 °C at different angles: (○) $\theta = 15°$ and (□) $\theta = 150°$.

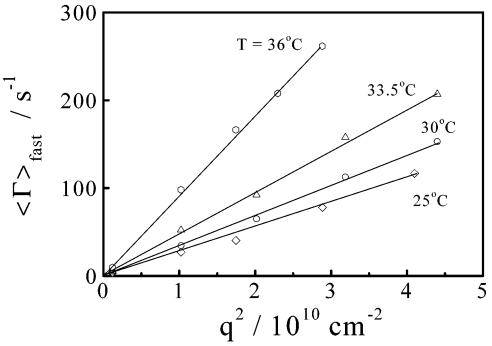

Figure 5. Scattering vector (q) dependence of the average characteristic linewidth ($\langle\Gamma\rangle_{fast}$) of the fast relaxation mode of core−shell particles in water.

perse, hard sphere, including the effect of backscattering, can be written as

$$g^{(1)}(t) = B_1 \exp(-q^2 \mathrm{D}t) + B_2 \exp(-q^{*2} \mathrm{D}t) \qquad (7)$$

and

$$\langle\Gamma\rangle_{slow} = \langle\Gamma\rangle_{fast}\left(\frac{q^{*2}}{q^2}\right) \qquad (8)$$

where $q^* = (4\pi n/\lambda_0) \sin[(180 - \theta)/2]$. Our results revealed that the plot of Γ vs q^{*2} is not a straight line passing through the origin. Moreover, $\langle\Gamma\rangle_{slow} \neq \langle\Gamma\rangle_{fast}(q^{*2}/q^2)$, which indicates that the slow mode does not stem from the refraction. Furthermore, after the chains are fully collapsed on the surface at 36 °C, the slow mode disappears. If it was due to the reflection, the slow mode should persist, even at 36 °C.

Before we discuss the nature of such a slow relaxation, let us first examine how these two relaxation modes are located in the space of the characteristic decay time. Figure 4 shows two distributions of the q^2-scaled characteristic linewidth (Γ/q^2) obtained from the Laplace inversion of two corresponding intensity−intensity time correlation functions, measured at low θ and large θ. It clearly shows that, with increasing θ, the narrow distribution of $G(\Gamma/q^2)$ values at $\theta = 15°$ splits into two well-separated peaks at $\theta = 150°$; however, the fast mode remains in almost the same position. This reveals that the fast relaxation at different θ has the same origin, namely, the translation diffusion of the entire particles.

Figure 5 shows that the scattering vector (q) dependence of the average linewidth $\langle\Gamma\rangle_{fast}$ (characteristic relaxation rate) of the fast mode, where $\langle\Gamma\rangle_{fast}$ was calculated from the relation

$$\langle\Gamma\rangle_{fast} = \int_{\Gamma_1}^{\Gamma_2} G(\Gamma) \exp(-\Gamma t)\, \mathrm{d}\Gamma$$

with Γ_1 and Γ_2 being the two boundary linewidths of each peak related to the fast mode in Figure 4. The plots of $\langle\Gamma\rangle_{fast}$ versus q^2 at different temperatures are straight lines passing through the origin, which is a characteristic of diffusive relaxation. As shown in Figure 3, the contribution of the slow mode decreases as the temperature increases (shrinkage of the grafted chains). As expected, the measured intensity−intensity time correlation functions of the core−shell particles with a fully collapsed shell at 36 °C have only one fast relaxation mode (translation diffusion), even at the highest measured scattering angle of $\theta = 154°$.

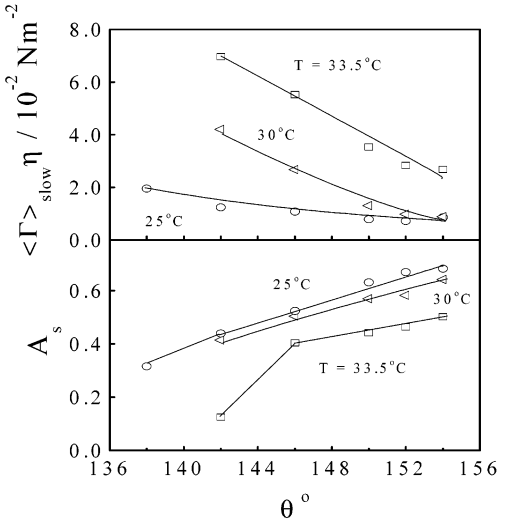

Figure 6. Scattering vector (q) dependence of the viscosity-corrected average characteristic linewidth ($\langle\Gamma\rangle_{slow}\eta$) and the intensity contribution of slow relaxation mode (A_s) of core−shell particles in water.

The translational diffusion of the center of mass of the core−shell particles is not interesting in the present study. Hereafter, we will focus on the slow relaxation mode related to the internal motions of the chains grafted on the PS core. It is known that the Laplace inversion of $|g^{(1)}(t,q)| = \int_0^\infty G(\tau)\ e^{-t/\tau}\ dt$ is an ill-conditioned mathematical problem, because of some inevitable experimental noise. The resultant linewidth distribution is extremely sensitive, even to noise as low as 0.1%. Therefore, to extract the average characteristic linewidth of the slow mode ($\langle\Gamma\rangle_{slow}$) reliably, we used a double exponential function, $G^{(2)}(t,q) \approx (A_f\ e^{-\langle\Gamma\rangle_{fast}t} + A_s\ e^{-\langle\Gamma\rangle_{slow}t})^2$, to fit each time correlation function, in which we fixed the value of $\langle\Gamma\rangle_{fast}$ for each temperature, which is related to the slope calculated from each line in Figure 5. Note that the sum of the intensity weightings (contributions) of the fast and slow relaxation modes (A_f and A_s) is equal to unity, i.e, $A_f + A_s = 1$. Therefore, the fitting actually is dependent only on two parameters, which makes us fairly confident in the fitting results. The error of such obtained $\langle\Gamma\rangle_{slow}$ is <10%, after taking into account all uncertainties. The quality of the fitting is also shown in the supplementary materials.

Figure 6 shows that, with an increasing scattering angle θ or a decreasing observation length ($1/q$), the intensity weighting of the slow relaxation increases, but the viscosity-corrected linewidth $\langle\Gamma\rangle_{slow}$ decreases (i.e., the motions become slower). Previous evanescent-wave dynamic-light-scattering studies of the polystyrene chains adsorbed on a flat glass surface showed that the slow relaxation was related to the local thermally agitated composition fluctuation of the swollen brush layer.[26] Based on this interpretation, the decrease of A_s is understandable, because local modes with a smaller wavelength are not observable when the observation length ($1/q$) is too long. On the other hand, Figure 6 shows that, for a given scattering angle, $\langle\Gamma\rangle_{slow}\eta$ increases, but A_s decreases, as the temperature increases, especially at lower θ. This means that the local motions become fast, but contribute less, when the grafted chains are in the shrunken state.

Qualitatively, at higher θ, the observation length becomes so much smaller that the light probes local motions of long PNIPAM chains that are densely grafted on the PS core. Note that the swollen grafted chains are forced to pack together and become entangled with each other. They are actually in the semidilute regime. At 25 °C, the swollen chains are extended away from the core, because of the exclusion. Therefore, the close packing in a limited space hinders the chain movements. The composition fluctuation slows. It has been shown that the Rouse-like diffusion leads to the characteristic q-insensitive relaxation, because the mean-squared fluctuation of the free chain ends in the perpendicular direction is proportional to the chain length. This explains the weak dependence of $\langle\Gamma\rangle_{slow}$ on q at 25 °C. The chain contraction should increase the space between two nearby chains, so that the motions of each chain will be less hindered. This might explain the increase of $\langle\Gamma\rangle_{slow}$ with increasing temperature. At 36 °C, the grafted chains fully collapse on the PS core, so that the chain density fluctuation in the shell is suppressed and the slow mode disappears at this temperature.

Figure 6 also shows that $\langle\Gamma\rangle_{slow}$ decreases as θ increases. It is helpful to note that, for linear chains in a good solvent and dilute regime, using a higher q value, one probes the internal motions with a shorter wavelength (high frequency). At 25 °C (good solvent), the relaxation rate is almost independent of the scattering vector. The stronger dependence on q occurs at 33.5 °C (poor solvent; the theta condition is ∼30.6 °C for free chains), at which temperature the chains might start to overlap with each other and enter the semidilute regime. Therefore, we should not attribute the detected slow motions to internal motions of individual grafted chains, but rather to the collective motion of the shell. On the other hand, Fytas et al.[26] attributed such a decrease of $\langle\Gamma\rangle_{slow}$ to the increase of the scattering intensity $I(q)$, because $\Gamma(q) = q^2\Omega g_1(q)/I(q)$, where Ω is the pure kinetic Onsager coefficient and $g_1(q)$ is the chain factor. We should not forget that, unlike the polymer chains that are free in semidilute solution, the size and density of the "blobs" of the grafted chains are not uniform. For example, no chain entanglement should occur near the core. As shown in Figure 1, when the temperature increases from 25 °C to 30 °C, the shrinking of the grafted chains is relatively small. The shrinking of the shell is expected to start from the periphery, i.e., the free chain end. The slowing of the relaxation with increasing temperature is less at higher θ (shorter observation lengths), which implies that the chain ends do contribute significantly to the slow relaxation mode. However, we cannot offer a definite explanation at this moment.

de Gennes[20] showed that the dynamics of an adsorbed polymer layer with a grafting density in the semidilute regime is determined by the balance between a restoring force due to the osmotic pressure gradient and a viscous force exerted on the polymer due to the motions of the grafted polymer chains, with respect to the background of solvent. The lowest breathing longitudinal relaxation rate was proportional to $q_0R_F^{-3}/\eta_0$, where q is the scattering vector, R_F the thickness of the adsorbed layer, and η_0 the viscosity of solvent. Farago et al.[25] and Fytas et al.[26] showed that, for a given grafting density, the estimate of the relaxation rate of the grafted chain can be scaled to the brush thickness $\langle L\rangle_{brush}$ as $\langle\Gamma\rangle_{slow} \approx \kappa T/(\eta_0\langle L\rangle_{brush}^{\alpha})$ with a predicated value of $\alpha = 3$. However, Figure 7 shows that $\langle\Gamma\rangle_{slow}\eta_0/T \approx \langle L\rangle_{brush}^{-2.5\pm0.2}$. It is helpful to note that the change of $\langle L\rangle_{brush}$ is rather limited. Such an obtained scaling exponent only tells us that the value of α is <3. Therefore, we should be too serious about the accuracy of its value. Fytas et al.[26] also found that the measured exponent α was <3. In our experiments, the decrease of $\langle L\rangle_{brush}$ and the increase of the chain density occur at the same time, with increasing temperature. It is expected that the increase in the chain density results in an increase of the friction, which should slow the relaxation. This is an additional effect on the rate of the slow relaxation, which might

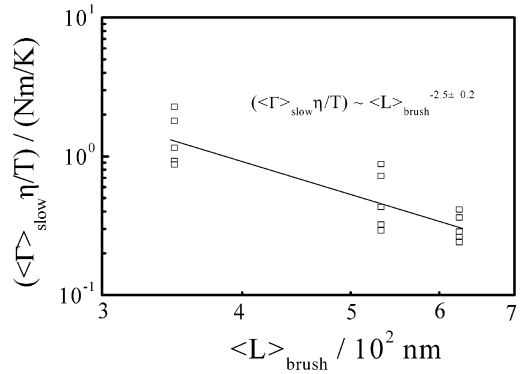

Figure 7. Shell thickness ($\langle L\rangle_{brush}$) dependence of the viscosity-corrected average characteristic linewidth ($\langle\Gamma\rangle_{slow}\eta$) of the slow relaxation of core−shell particles in water.

explain why the observed value of α is <3. The computer simulation indicated that α is in the range of 2.4−3.1, with a varying grafting density.[22]

Conclusion

There is some slow dynamics of long polymer chains densely grafted on a surface, which is only observed at higher scattering angles (shorter observation length in laser-light scattering). Such slow relaxation is related to density fluctuation of the grafted chains (breath mode) along the radial direction (perpendicular to the surface). The relaxation slows and contributes less to the scattered-light intensity as the chain shrinks, especially at a relatively short observation length. For a given temperature (chain conformation), the relaxation becomes faster and contributes more and more to the scattered-light intensity as the observation length decreases. The viscosity-corrected relaxation rate (linewidth, $\langle\Gamma\rangle_{slow}$) is scalable to the brush thickness $\langle L\rangle_{brush}$ as $\langle\Gamma\rangle_{slow} \propto \langle L\rangle_{brush}^{-\alpha}$, with $\alpha = 2.5 \pm 0.2$, which is smaller than the predicated value of 3; this might be due to the increase of the chain density with decreasing brush thickness when the chain shrinks. The fitting of each scattering intensity profile with a core−shell mode shows that the chain density profile of the shell can be described as $\rho(r) = \rho_0 r^{-1}$ in the range of $R_c \le r \le R$, where R_c and R are the radii of the core and the particle, respectively. The chain density at the core surface changes from 7.3×10^{-3} g/cm^3 to 7.2×10^{-2} g/cm^3 when the temperature increases from 25 °C to 36 °C.

Acknowledgment. The financial support of the Hong Kong Special Administration Region Earmarked Grants (Nos. CUHK4025/02P, 2160181), the Special Funds for Major State Basic Research Projects (No. G1999064800), the BASF−Germany−Sino Research & Development Fund, and the National Natural Science Foundation (NNSF) of China (Nos. 2003/2005, 20274045) is gratefully acknowledged.

Supporting Information Available: Laplace inversion (CONTIN) fitting of two measured intensity−intensity time correlation functions, where the lines are fitting results (PDF). This material is available free of charge via the Internet at http://pubs.acs.org.

References and Notes

(1) Alexander, S. J. *J. Phys. (Paris)* **1977**, *38*, 983−987.
(2) de Gennes, P. G. *Macromolecules* **1980**, *13*, 1069−1075.
(3) Milner, S. T.; Witten, T. A. *Macromolecules* **1988**, *21*, 2610−2619.
(4) Zhulina, E. B.; Borisov, O. V.; Pryamitsyn, V. A.; Birshtein, T. M. *Macromolecules* **1991**, *24*, 140−149.
(5) Daoud, M.; Cotton, J. P. *J. Phys. (Paris)* **1982**, *43*, 531−538.
(6) Stuart, M. A. C.; Waajen, F. H. W. H.; Cosgrove, T.; Vincent, B.; Crowley, T. L. *Macromolecules* **1984**, *17*, 1825−1830.
(7) Cosgrove, T.; Heath, T.; Lent, B.; Leermakers, F.; Scheutjens, J. *Macromolecules* **1987**, *20*, 1692−1696.
(8) Soga, K. G.; Guo, H.; Zuckermann, M. J. *Europhys. Lett*. **1995**, *29*, 531−536.
(9) Besold, G.; Guo, H.; Zuckermann, M. J. *J. Polym. Sci., Part B: Polym. Phys.* **2000**, *38*, 1053−1068.
(10) Stoyanov, S. D.; Paunov, V. N.; Kuhn, H.; Rehage, H. *Macromolecules* **2003**, *36*, 5032−5038.
(11) Hadziioannou, G.; Patel, S.; Granick, S.; Tirrell, M. *J. Am. Chem. Soc*. **1986**, *108*, 2869−2876.
(12) Ortega-Vinuesa, J. L.; Martín-Rodríguez, A.; Hidalgo-Álvarez, R. *J. Colloid Interface Sci*. **1996**, *184*, 259−267.
(13) Zhu, P. W.; Napper, D. H. *J. Colloid Interface Sci*. **1996**, *177*, 343−352.
(14) Förster, S.; Wenz, E.; Lindner, P. *Phys. Rev. Lett*. **1996**, *77*, 95−98.
(15) Hu, T.; Wu, C. *Phys. Rev. Lett*. **1999**, *83*, 4105−4107.
(16) Kidoaki, S.; Ohya, S.; Nakayama, Y.; Matsuda, T. *Langmuir* **2001**, *17*, 2402−2407.
(17) Lemieux, M.; Minko, S.; Usov, D.; Stamm, M.; Tsukruk, V. V. *Langmuir* **2003**, *19*, 6162.
(18) Lemieux, M.; Usov, D.; Minko, S.; Stamm, M.; Shulha, H.; Tsukruk, V. V. *Macromolecules* **2003**, *36*, 7244−7255.
(19) Yim, H.; Kent, M. S.; Huber, D. L.; Satija, S.; Majewski, J.; Smith, G. S. *Macromolecules* **2003**, *36*, 5244−5251.
(20) de Gennes, P. G. *Adv. Colloid Interface Sci*. **1987**, *27*, 189−209.
(21) Halperin, A.; Alexander, S. *Europhys. Lett*. **1988**, *6*, 329−334.
(22) Murat, M.; Grest, G. S. *Macromolecules* **1989**, *22*, 4054−4059.
(23) Klushin, L. I.; Skvortsov, A. M. *Macromolecules* **1991**, *24*, 1549−1553.
(24) Halperin, A.; Tirrell, M.; Lodge, T. P. *Adv. Polym. Sci*. **1992**, *100*, 31−71.
(25) Farago, B.; Monkenbush, M.; Richter, D.; Huang, J. S.; Fetters, L. J.; Gast, A. P. *Phys. Rev. Lett*. **1993**, *71*, 1015−1018.
(26) Fytas, G.; Anastasiadis, S. H.; Seghrouchni, R.; Viassopoulos, D.; Li, J.; Factor, B. J.; Theobald, W.; Toprakcioglu, C. *Science* **1996**, *274*, 2041−2044.
(27) Seghrouchni, R.; Petekidis, G.; Vlassopoulos, D.; Fytas, G.; Semenov, A. N.; Roovers, J.; Fleischer, G. *Europhys. Lett*. **1998**, *42*, 271−276.
(28) Semenov, A. N.; Viassopoulos, D.; Fytas, G.; Vlachos, G.; Fleischer, G.; Roovers, J. *Langmuir* **1999**, *15*, 358−368.
(29) Sigel, R.; Pispas, S.; Vlassopoulos, D.; Hadjichristidis, N.; Fytas, G. *Phys. Rev. Lett*. **1999**, *88*, 4666−4669.
(30) Zhao, B.; Brittain, W. J. *Prog. Polym. Sci*. **2000**, *25*, 677−710.
(31) Perruchot, C.; Khan, M. A.; Kamittsi, A.; Armes, S. P.; Werne, T. V.; Patten, T. E. *Langmuir* **2001**, *17*, 4479−4481.
(32) Kizhakkedathu, J. N.; Norris-Jones, R.; Brooks, D. E. *Macromolecules* **2004**, *37*, 734−743.
(33) Jayachandran, K. N.; Takacs-Cox, A.; Brooks, D. E. *Macromolecules* **2002**, *35*, 4247−4257.
(34) Chu, B. *Laser Light Scattering*, 2nd Edition; Academic Press: New York, 1991.
(35) Bantle, S.; Schmidt, M.; Burchard, W. *Macromolecules* **1982**, *15*, 1604.